Electronic Supplementary Information (ESI)

for

Ultra-Small Carbon Nanospheres (< 50 nm) of Uniform Tunable Sizes by a Convenient Catalytic Emulsion Polymerization Strategy: Superior Supercapacitive and Sorption Performances

Vimal K. Tiwari,[a] Zhe Chen,[a] Fan Gao,[b] Zhiyong Gu,[b] Xueliang Sun,[c] and Zhibin Ye [a,*]

a. Bharti School of Engineering, Laurentian University, Sudbury, Ontario P3E 2C6, Canada

b. Department of Chemical Engineering, University of Massachusetts, Lowell, Massachusetts 01854, United States

c. Department of Mechanical and Materials Engineering, Western University, London, Ontario N6A 5B9, Canada

* Corresponding author; Email: zye@laurentian.ca

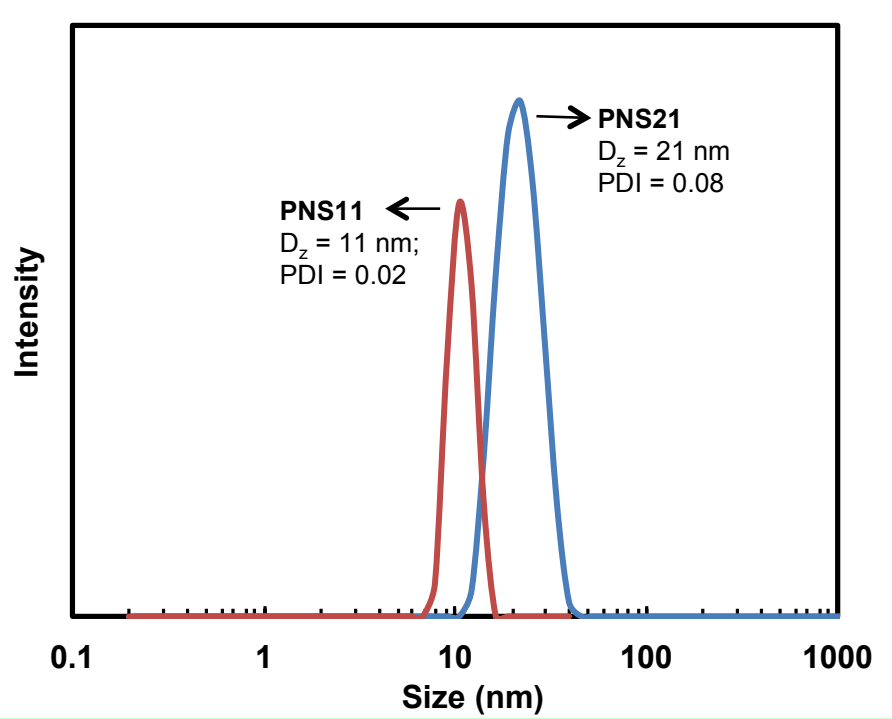

Figure S1. DLS particle size distribution of the polymer nanospheres (PNS11 and PNS21) obtained by the miniemulsion polymerization.

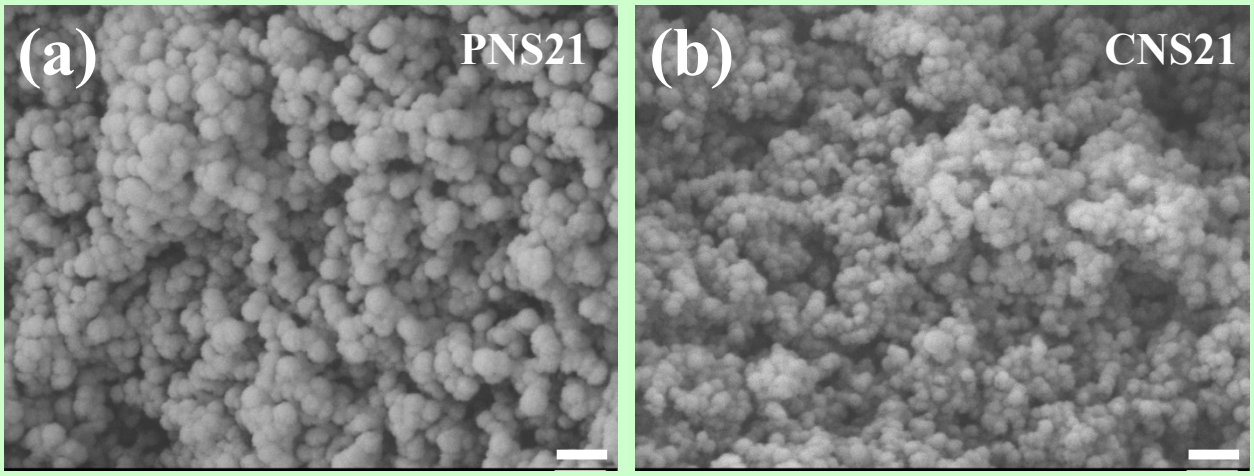

Figure S2. SEM images of PNS21 after hydrothermal treatment and CNS21. Scale bar = 100 nm. The PNS21 sample was gold-coated for SEM imaging.

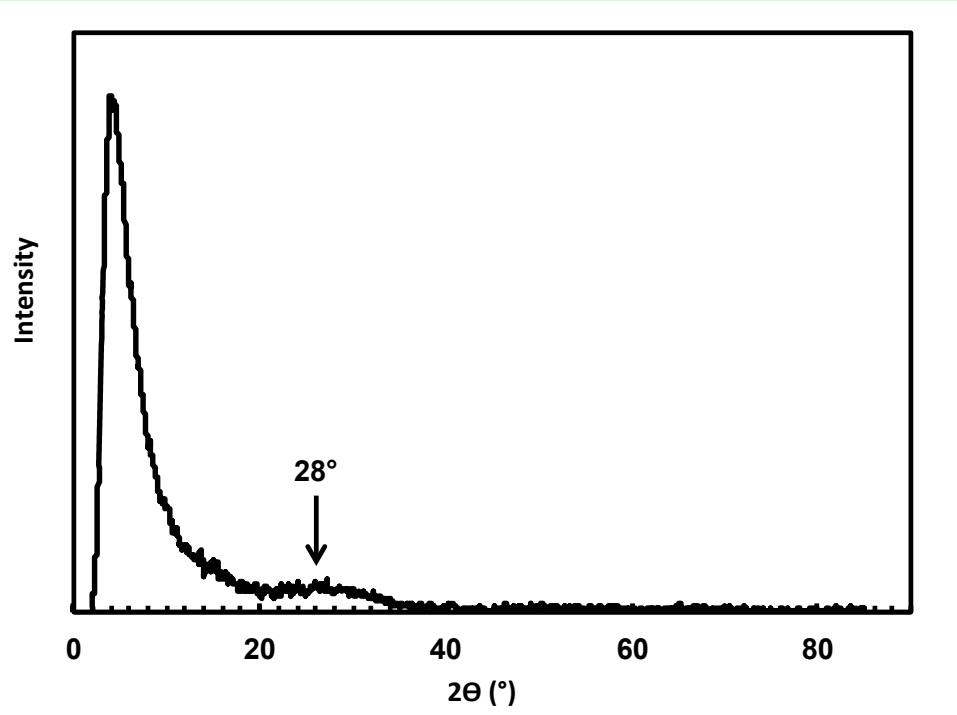

Figure S3. XRD pattern of CNS21.

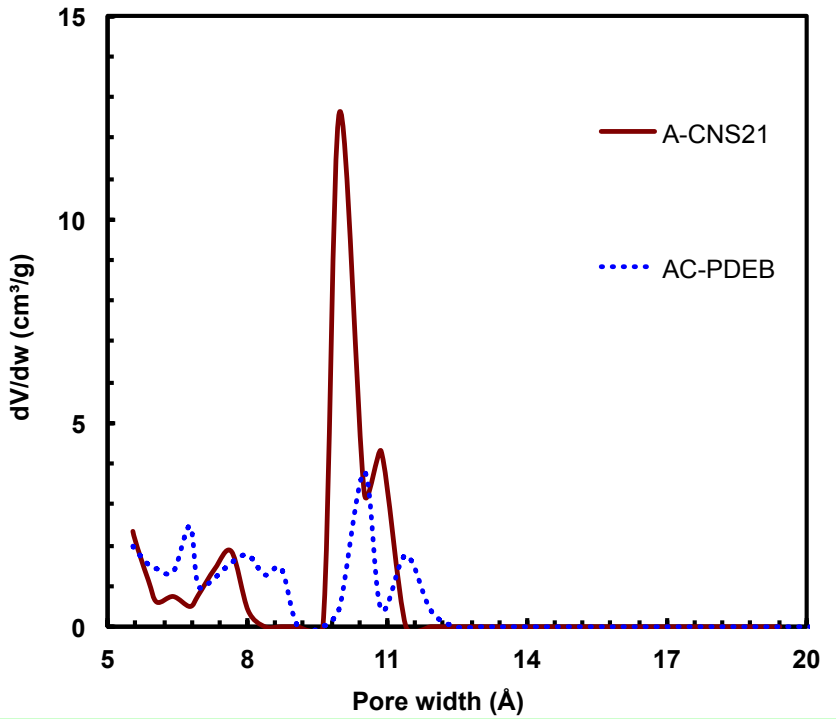

Figure S4. Micropore size distribution curves of A-CNS21 and AC-PDEB determined with NLDFT model.

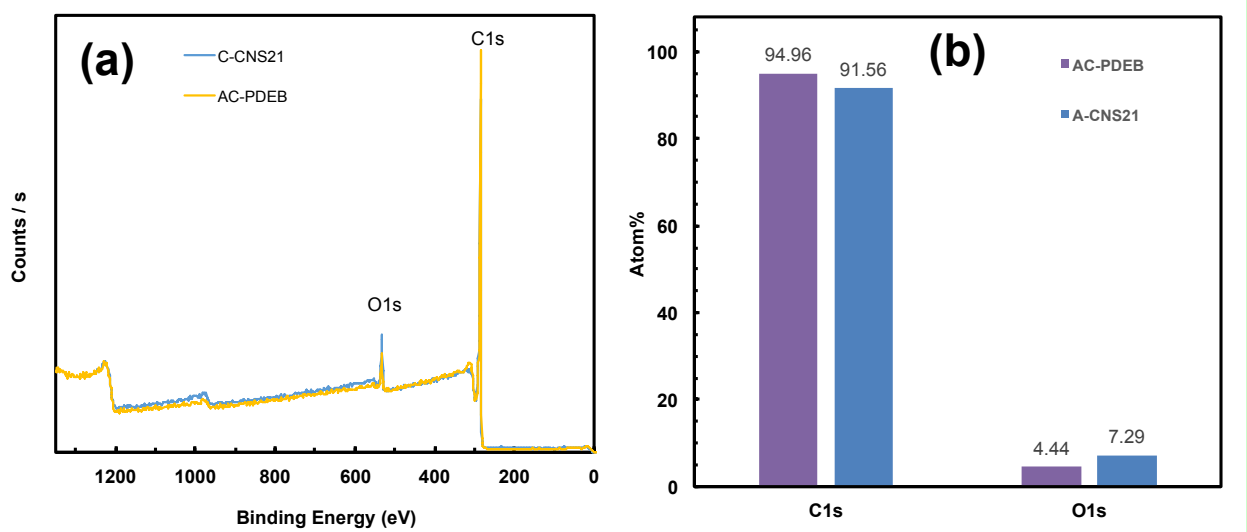

Figure S5. XPS survey spectra (a) and elemental compositions (b) of A-CNS21 and AC-PDEB.

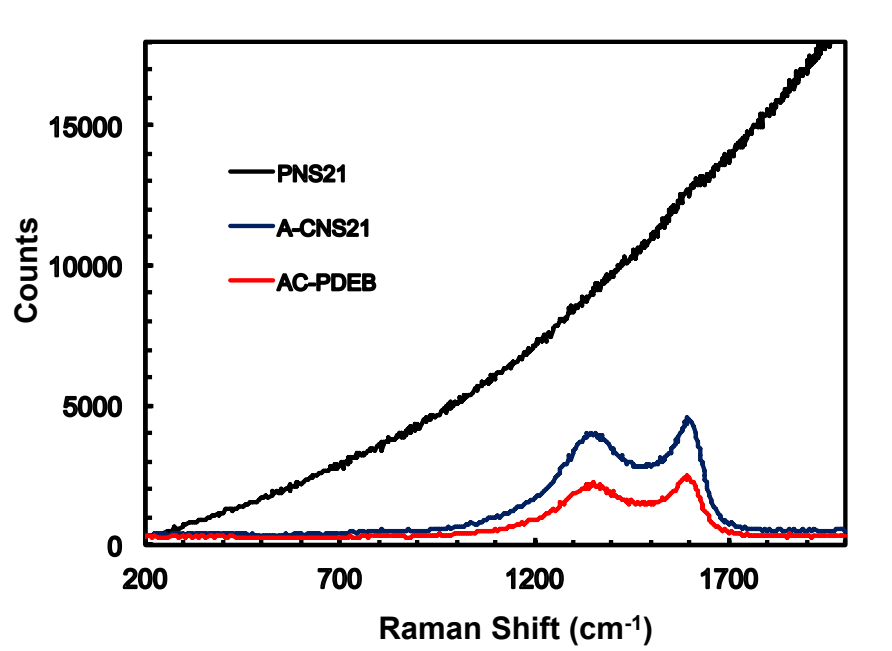

Figure S6. Raman spectra of PNS21 (after hydrothermal treatment), A-CNS21 and AC-PDEB.

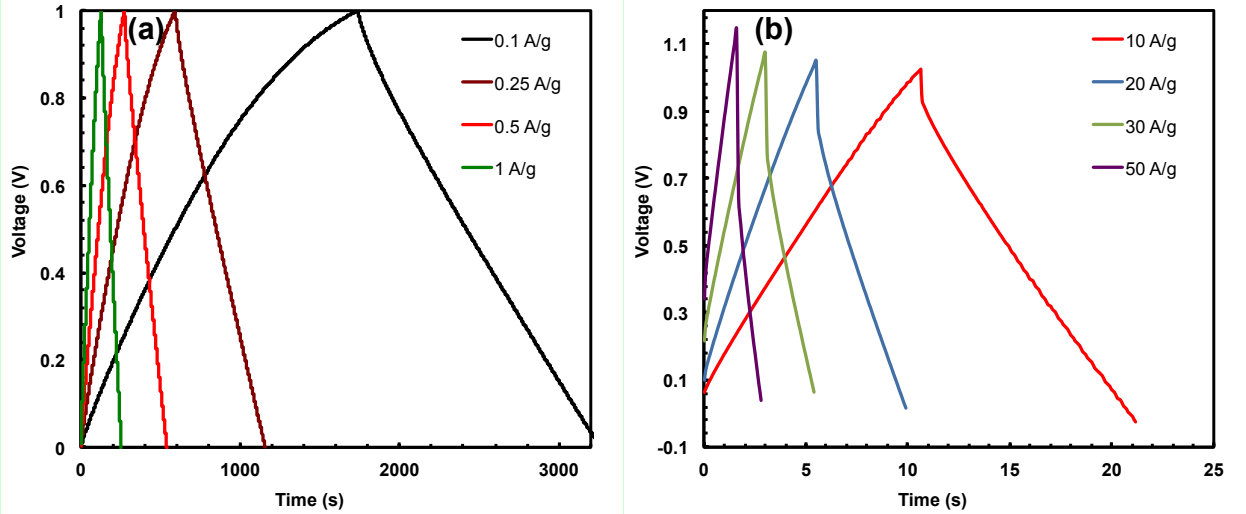

Figure S7. GCD curves of A-CNS21 in a two-electrode cell configuration in 1.0 M H_2SO_4 at different current densities within (a) 0.1–1 A/g; (b) 10–50 A/g.

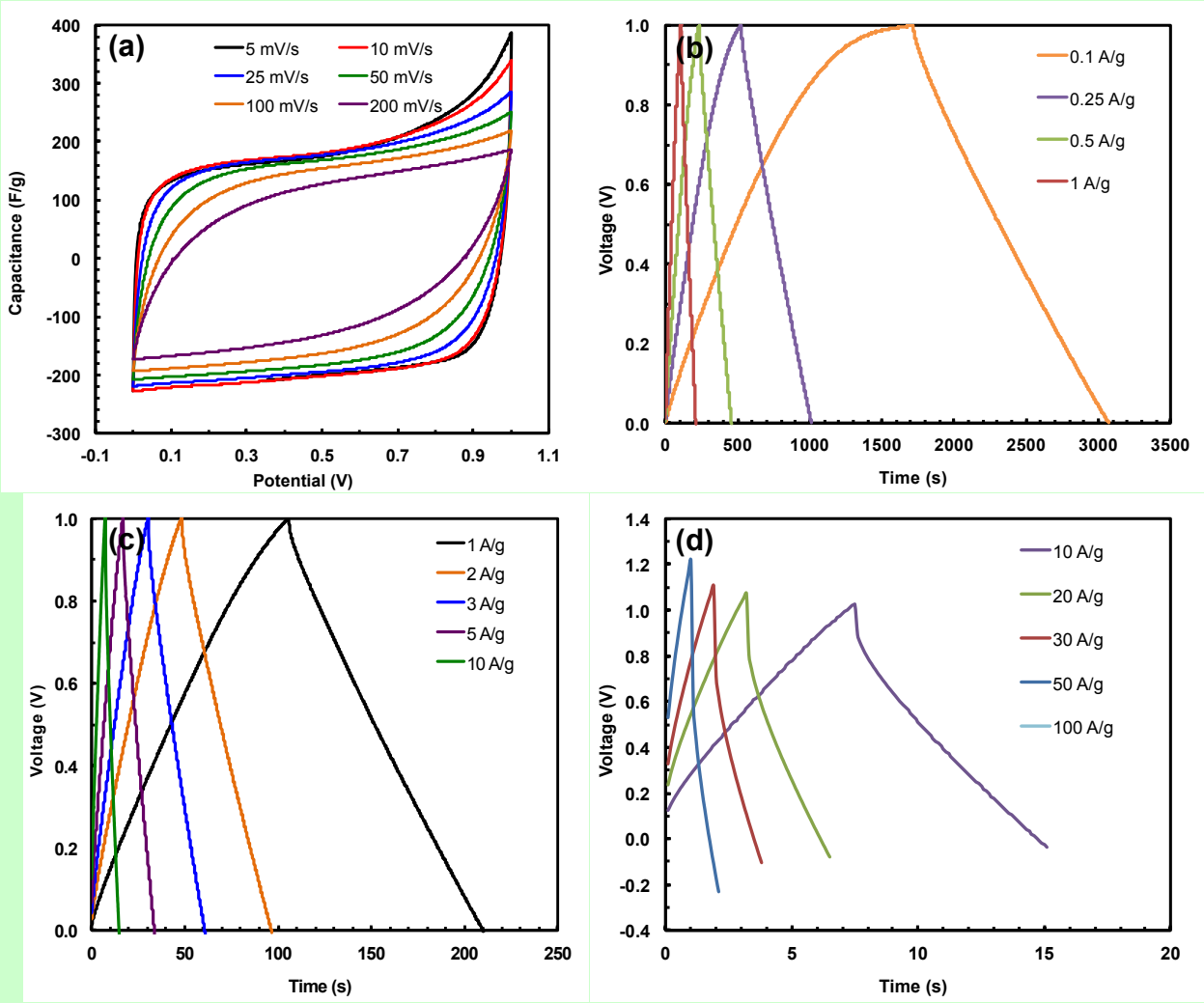

Figure S8. Electrochemical supercapacitive results of AC-PDEB in a two-electrode cell configuration in 1 M H_2SO_4 aqueous electrolyte: (a) CV curves at different voltage sweep rates; (b) GCD curves at different current densities within (b) 0.1–1 A/g, (c) 1–10 A/g, and (d) 10–100 A/g.

Table S1. Summary of supercapacitive performances of representative porous carbon electrodes in a two-electrode symmetrical cell configuration with aqueous electrolyte.

Sample		Current density range	Reference data			Data from this work with A-CNS21	
			Capacitance (F/g) at initial current density	Capacitance retention (%) at final current density	Ref.	Capacitance (F/g) at initial current density	Capacitance retention (%) at final current density
Porous carbon spheres	Polystyrene-based hierarchical porous carbon spheres	5–50 mV/s	185 [a]	89 [a]	1	**223**	**93.7**
	Mesoporous size controllable carbon microspheres	1–20 A/g	268 [a]	60.8 [a]	2	**255**	**82.0**
	Highly porous carbon spheres	5–100 mV/s	169	83	3	**223**	**89.7**
	Nitrogen-doped carbon microspheres from organic frameworks	0.2–20 A/g	282 [a]	55 [a]	4	**283** (@0.25 A/g)	**74** (20 A/g)
	Mesoporous carbon nanospheres	10–200 mV/s	185	75	5	**223**	**74.9**
	Carbon spheres with microporous structure	5–50 mV/s	~182	70	6	**223**	**93.7**
	Hierarchcally porous carbon spheres by hydrothermal method	0.1–10 A/g	170	82	7	**305**	**71.8**
	Carbon microspheres	0.1–20 A/g	241	80	8	**305**	**68.5**
Hollow carbon spheres	Ultrahigh-surface- area hollow carbon nanospheres	0.5–10 A/g 5–50 mV/s	~185 201	81.8 92.9	9	**268** **223**	**81.7** **93.7**
	Porous nitrogen-doped hollow carbon spheres	0.5–10 A/g	213 [a]	55.6 [a]	10	**268**	**81.7**
	Hierarchical porous carbon hollow spheres	0.5–10 A/g	270 [a]	72.8 [a]	11	**268**	**81.7**
	Carbon nanocages (CNC700)	0.1–10 A/g	260	68.4	12	**305**	**71.8**
	Nitrogen-doped carbon nanocages	1–50 A/g	313	75	13	**255**	**75.3**
	Carbon nano-onions	0.75–25 A/g	126.3	71	14	**268** (at 0.5 A/g)	**75** (at 30 A/g)
Mesoporous carbons	Porous carbon with small mesopores	0.1–50 A/g	425	~66	15	**305**	**63.0**
Carbon aerogels	Magnetite carbon aerogels	5–100 mV/s 0.5–6 A/g	369.2 [a] 337.2 [a]	38.5 [a] 65.9 [a]	16	**223** **268** (at 0.5 A/g)	**89.7** **81.7** (at 10 A/g)

	Mesoporous carbon/graphene aerogels	0.5–10 A/g	197 [a]	71.6 [a]	17	**268**	**81.7**
Hierarchically porous carbons	Hierarchically porous carbons (CNB-3)	0.5–20 A/g	247 [a]	67.6 [a]	18	**268**	**78.0**
	3D microporous conducting carbon beehive	0.5–30 A/g	254	55	19	**268**	**75.3**
	Porous carbon from metal-organic framework	5–50 mV/s	204	77.9	20	**223**	**93.7**
	Nitrogen-doped ordered nanoporous carbons	0.1–10 A/g	~270	47	21	**305**	**71.8**
	Hierarchical carbide-derivde carbon foams	1–20 A/g	240	72.9	22	**255**	**82.0**
Graphene/ CNTs	Microporous carbon nanoplates	0.1–52.5 A/g	264	120	23	**305**	**63.0** (at 50 A/g)
	Mesoporous graphene-like carbon sheet	5–200 mV/s	~255 [a]	~78 [a]	24	**233**	**78.0**
	3D N-doped graphene-CNT networks	0.5–5 A/g	180	52.8	25	**268**	**85.4**
	Porous graphene carbons	1–20 A/g	280	~46	26	**255**	**82.0**
	2D porous carbon nanosheets	1–20 A/g	228	89	27	**255**	**82.0**
	Holey graphene frameworks	1–50 A/g	310	82	28	**255**	**75**
	Microporous carbon nanosheets	0.5–10 A/g	213 [a]	75.1 [a]	29	**268**	**81.7**
	Functionalized graphene hydrogel	1–20 A/g	441	80	30	**255**	**82.0**
	Graphene and CNT foam	5–100 mV/s	270	80	31	**223**	**89.7**
	Graphene-based frameworks	5–100 mV/s	175	47	32	**223**	**89.7**
	GO/MWCNT composites	5–100 mV/s	251 [a]	30 [a]	33	**223**	**89.7**
	GO reduced by urea	0.5–30 A/g	255 [a]	29 [a]	34	**268**	**75.3**
Carbons from biomass	Dead leaves derived carbons	0.5–10 A/g	401	64	35	**268**	**81.7**
	Carbonized chicken eggshell membranes with 3D architecture	0.2–20 A/g	297 [a]	66 [a]	36	**283** (at 0.25 A/g)	**73.9** (20 vs. 0.25 A/g)

[a] Data obtained in a 3-electrode cell configuration, where the specific capacitance data are often significantly higher than the corresponding ones obtained in a 2-electrode symmetrical cell at the same current density (see Ref. 37).

Table S2. Summary of adsorption capacities of representative porous materials toward toluene and methanol vapors at 25 ºC.

Sample		Toluene		Methanol		Reference
		Relative vapor pressure	Adsorption capacity (mg/g)	Relative vapor pressure	Adsorption capacity (mg/g)	
A-CNS21		0.01 0.05 0.1 0.99	159 585 866 967	0.01 0.05 0.1 0.99	21 167 366 937	This work
AC-PDEB		0.01 0.05 0.1 0.99	38 163 366 631	0.01 0.05 0.1 0.99	46 250 380 572	This work
Porous carbons	Ultrahigh-surface-area hollow carbon nanospheres (HCN-900-20H2R)	0.1 0.9	~ 800 1500	0.1 0.9	~ 240 1230	9
	Single-walled carbon nanotubes (CVD80)	0.1 0.94	~160 456			38
	Activated grahene aerogel	0.1 1	~130 710	0.1 1	~40 641	39
	Activated carbon	1	640			40
	Hierarchical porous carbon microfibers	0.9	243			41
	Activated carbon fiber cloth	0.1 0.9	560 (20ºC) 600 (20ºC)			42
Porous polymers	Porous aromatic framework (PAF-1)	0.1 1	~800 1357			43
	Porous aromatic framework (PAF-5)	0.1 1	482 1061	0.1 1	81 933	44
	Porous aromatic framework (PAF-11)	0.1 1	~300 780	0.1 1	~65 654	45
	Porous polymeric nanoscale networks			0.1 0.9	~82 741	46
	Mesoporous conjugated polycarbazole (CPOP-9)	0.1 1	~200 1355			47
	Porous conjugated polyporphyrins (CPOP-12)	0.1 1	~400 1192	0.1 1	~160 766	48
	Microporous polymeric microsphere	0.08 1	~360 887	0.08 1	~100 574	49
MOF	HKUST-1	0.06 0.9	~608 620			50
	MIL-101	0.08 0.9	~239 1389			51
	$PdCl_2$/MIL-101	0.06 0.9	660 1285			51
	$[Zn_4O(bdc)(bpz)_2]$•4DMF•$6H_2O$	0.1 0.9	510 ~550	0.08 0.2 0.9	25 420 ~480	52
	$[Cu_2(bdc)_2(DMF)]$ •H_2O•$(DMF)(C_2H_5OH)_{0.5}$			0.1 0.9	~90 171	53

Table S3. Summary of CO_2 adsorption capacity (at 0 ºC and 1 bar) of most representative porous carbons.

Sample	CO_2 adsorption		Reference
	Adsorption capacity (wt%)	CO_2/N_2 selectivity (mol/mol)	
A-CNS21	26	11	This work
AC-PDEB	28	11	This work
Carbon microspheres	15.8		8
Monodisperse carbon spheres	19.2		54
Highly microporous carbon spheres	29		55
Activated carbon molecular sieves from petroleum pitch (VR-5-M)	38	2.8	56
Activated carbon molecular sieves from petroleum pitch (VR-93-M)	24	14	56
Phenolic resin-based activated carbon spheres (CS*-P-A)	39		57
Carbide derived carbon	31		58
Purified SWCNTs	22		59
Activated carbon	16		60
Activated carbon fibres	14		61
Activated carbon	12		62
Activated carbon	11		59
Nitrogen enriched porous carbon spheres	27		63

Table S4. Summary of H_2 adsorption capacity (at 77 K and 1 bar) of most representative porous carbons.

Sample	H_2 adsorption capcity (wt%)	Reference
A-CNS21	2.5	This work
AC-PDEB	2.4	This work
Activated carbon	2.49	64
Biomass waste-derived microporous carbons	2.55	65
MOF-derived hierarchically porous carbons	3.25	66
Activated carbon (AC Norit 990293)	2.1	67
TiC carbide-derived carbon	3.0	68
Single-walled carbon nanotubes	0.924	69
Multi-walled carbon nanotubes	ca. 0.2	68
Superactivated carbide-derived carbons	2.7	70
MOF-derived nanoporous carbon (C1000)	2.77	71
Carbon hollow spheres	1.1–1.5	72

References

1. Xu, F.; Cai, R.; Zeng, Q.; Zou, C.; Wu, D.; Li, F.; Lu, X. Liang, Y.; Fu, R. Fast ion transport and high capacitance of polystyrene-based hierarchical porous carbon electrode material for supercapacitors. *J. Mater. Chem.* **2011**, *21*, 1970–1976.
2. Ma, X.; Gan, L.; Liu, M.; Tripathi, P. K.; Zhao, Y.; Xu, Z.; Zhu, D.; Chen, L. Mesoporous size controllable carbon microspheres and their electrochemical performances for supercapacitor electrodes. *J. Mater. Chem. A* **2014**, *2*, 8407–8415.
3. Zhang, C.; Hatzell, K. B.; Boota, M.; Dyatkin, B.; Beidaghi, M.; Long, D.; Qiao, W.; Kumbur, E. C.; Gogotsi, Y. Highly porous carbon spheres for electrochemical capacitors and capacitive flowable suspension electrodes. *Carbon* **2014**, *77*, 155–164.
4. Han, J.; Xu, G.; Dou, H.; MacFarlane, D. R. Porous nitrogen-doped carbon microspheres derived from microporous polymeric organic frameworks for high performance electric double-layer capacitors. *Chem. Eur. J.* **2015**, *21*, 2310–2314.
5. Lei, Z.; Christov, N.; Zhang, L. L.; Zhao, X. S. Mesoporous carbon nanospheres with an excellent electrocapacitive performance. *J. Mater. Chem.* **2011**, *21*, 2274–2281.
6. Tanaka, S.; Nakao, H.; Mukai, T.; Katayama, Y.; Miyake, Y. An experimental investigation of the ion storage/transfer behavior in an electrical double-layer capacitor by using monodisperse carbon spheres with microporous structure. *J. Phys. Chem. C* **2012**, *116*, 26791–26799.
7. Gong, Y.; Wei, Z.; Wang, J.; Zhang, P.; Li, H.; Wang, Y. Design and fabrication of hierarchically porous carbon with a template-free method. *Sci. Rep.* **2014**, *4*, 6349.
8. Wang, J.; Yao, L.; Ma, C.; Guo, X.; Qiao, W.; Ling, L.; Long, D. Organic amine-mediated synthesis of polymer and carbon microspheres: mechanism insight and energy-related applications. *ACS Appl. Mater. Interfaces* **2016**, *8*, 4851–4861.
9. Xu, F.; Tang, Z.; Huang, S.; Chen, L.; Liang, Y.; Mai, W.; Zhong, H.; Fu, R.; Wu, D. Facile synthesis of ultrahigh-surface-area hollow carbon nanospheres for enhanced adsorption and energy storage. *Nature Commun.* **2014**, *6*, 7221.
10. Han, J.; Xu, G.; Ding, B.; Pan, J.; Dou, H.; MacFarlane, D. R. Porous nitrogen-doped hollow carbon spheres derived from polyaniline for high performance supercapacitors. *J. Mater. Chem. A* **2014**, *2*, 5352–5357.
11. Han, Y.; Dong, X.; Zhang, C.; Liu, S. Hierarchical porous carbon hollow-spheres as a high performance electrical double-layer capacitor material. *J. Power Sources* **2012**, *211*, 92–96.
12. Xie, K.; Qin, X.; Wang, X.; Wang, Y.; Tao, H.; Wu, Q.; Yang, L.; Hu, Z. Carbon nanocages as supercapacitor electrode materials. *Adv. Mater.* **2012**, *24*, 347–352.
13. Zhao, J.; Lai, H.; Lyu, Z.; Jiang, Y.; Xie, K.; Wang, X.; Wu, Q.; Yang, L.; Jin, Z.; Ma, Y.; Liu, J.; Hu, Z. Hydrophilic hierarchical nitrogen-doped carbon nanocages for ultrahigh supercapacitive performance. *Adv. Mater.* **2015**, *27*, 3541–3545.
14. Gao, Y.; Zhou, Y. S.; Qian, M.; He, X. N.; Redepenning, J.; Goodman, P.; Li, H. M.; Jiang, L.; Lu, Y. F. Chemical activation of carbon nano-onions for high-rate supercapacitor electrodes. *Carbon* **2013**, *51*, 52–58.
15. Kang, D.; Liu, Q.; Gu, J.; Su, Y.; Zhang, W.; Zhang, D. "Egg-box"-assisted fabrication of porous carbon with small mesopores for high-rate electric double layer capacitors. *ACS Nano* **2015**, *9*, 11225–11233.
16. Wu, X.-L.; Wen, T.; Guo, H.-L.; Yang, S.; Wang, X.; Xu, A.-W. Biomass-derived sponge-like carbonaceous hydrogels and aerogels for supercapacitors. *ACS Nano* **2013**, *7*, 3589–3597.

17. Liu, R.; Wan, L.; Liu, S.; Pan, L.; Wu, D.; Zhao, D. An interface-induced co-assembly approach towards ordered mesoporous carbon/graphene aerogel for high-performance supercapacitors. *Adv. Funct. Mater.* **2015**, *25*, 526–533.
18. Guo, D.-C.; Mi, J.; Hao, G.-P.; Dong, W.; Xiong, G.; Li, W.-C.; Lu, A.-H. Ionic liquid C_{16}mimBF_4 assisted synthesis of poly(benzoxazine-*co*-resol)-based hierarchically porous carbons with superior performance in supercapacitors. *Energy Environ. Sci.* **2013**, *6*, 652–659.
19. Puthusseri, D.; Aravindan, V.; Madhavi, S.; Ogale, S. 3D micro-porous conducting carbon beehive by single step polymer carbonization for high performance supercapacitors: the magic of in situ porogen formation. *Energy Environ. Sci.* **2014**, *7*, 728–735.
20. Liu, B.; Shioyama, H.; Akita, T.; Xu, Q. Metal-organic framework as a template for porous carbon synthesis. *J. Am. Chem. Soc.* **2008**, *130*, 5390–5391.
21. Liang, Y.; Liu, H.; Li, Z.; Fu, R.; Wu, D. In situ polydopamine coating-directed synthesis of nitrogen-doped ordered nanoporous carbons with superior performance in supercapacitors. *J. Mater. Chem. A* **2013**, *1*, 15207–15211.
22. Oschatz, M.; Borchardt, L.; Pinkert, K.; Thieme, S.; Lohe, M. R.; Hoffmann, C.; Benusch, M.; Wisser, F. M.; Ziegler, C.; Giebeler, L.; Rümmeli, M. H.; Eckert, J.; Eychmüller, A.; Kaskel, S. *Adv. Energy Mater.* **2014**, *4*, 1300645.
23. Yun, Y. S.; Cho, S. Y.; Shim, J.; Kim, B. H.; Chang, S.-J.; Baek, S. J.; Huh, Y. S.; Tak, Y.; Park, Y. W.; Park, S.; Jin, H.-J. Microporous carbon nanoplates from regenerated silica proteins for supercapacitors. *Adv. Mater.* **2013**, *25*, 1993–1998.
24. Zhang, P.; Qiao, Z.-A.; Zhang, Z.; Wan, S.; Dai, S. Mesoporous graphene-like carbon sheet: high-power supercapacitor and outstanding catalyst support. *J. Mater. Chem. A* **2014**, *2*, 12262–12269.
25. You, B.; Wang, L.; Yao, L.; Yang, J. Three dimensional N-doped graphene-CNT networks for supercapacitors. *Chem. Commun.* **2013**, *49*, 5016–5018.
26. Huang, J.; Wang, J.; Wang, C.; Zhang, H.; Lu, C.; Wang, J. Hierarchical porous graphene carbon-based supercapacitors. *Chem. Mater.* **2015**, *27*, 2107–2113.
27. Fan, X.; Yu, C.; Yang, J.; Ling, Z.; Hu, C.; Zhang, M.; Qiu, J. A layered-nanospace-confinment strategy for the synthesis of two-dimensional porous carbon nanosheets for high-rate performance supercapacitors. *Adv. Energy Mater.* **2015**, *5*, 1401761.
28. Xu, Y.; Lin, Z.; Zhong, X.; Huang, X.; Weiss, N. O.; Huang, Y.; Duan, X. Holey graphene frameworks for highly efficient capacitive energy storage. *Nature Commun.* **2014**, *5*, 4554.
29. Jin, Z.-Y.; Lu, A.-H.; Xu, Y.-Y.; Zhang, J.-T.; Li, W.-C. Ionic liquid-assisted synthesis of microporous carbon nanosheets for use in high rate and long cycle life supercapacitors. *Adv. Mater.* **2014**, *26*, 3700–3705.
30. Xu, Y.; Lin, Z.; Huang, X.; Wang, Y.; Huang, Y.; Duan, X. Functionalized graphene hydrogel-based high-performance supercapacitors. *Adv. Mater.* **2013**, *25*, 5779–5784.
31. Wang, W.; Guo, S.; Penchev, M.; Ruiz, I.; Bozhilov, K. N.; Yan, D.; Ozkan, M.; Ozkan, C. Z. Three dimensional few layer graphene and carbon nanotube foam architectures for high fidelity supercapacitors. *Nano Energy* **2013**, *2*, 294–303.
32. Wu, Z.-S.; Sun, Y.; Tan, Y.-Z.; Yang, S.; Feng, X.; Müllen, K. Three-dimensional graphene-based macro- and mesoporous frameworks for high-performance electrochemical capacitive energy storage. *J. Am. Chem. Soc.* **2012**, *134*, 19532–19535.

33. Aboutalebi, S. H.; Chidembo, A. T.; Salari, M.; Konstantinov, K.; Wexler, D.; Liu, H. K.; Dou, S. X. Comparison of GO, GO/MWCNTs composite and MWCNTs as potential electrode materials for supercapacitors. *Energy Environ. Sci.* **2011**, *4*, 1855–1865.
34. Lei, Z.; Lu, L.; Zhao, X. S. The electrocapacitive properties of graphene oxide reduced by urea. *Energy Environ. Sci.* **2012**, *5*, 6391–6399.
35. Biswal, M.; Banerjee, A.; Deo, M.; Ogale, S. From dead leaves to high energy density supercapacitors. *Energy Environ. Sci.* **2013**, *6*, 1249–1259.
36. Li, Z.; Zhang, L.; Amirkhiz, B. S.; Tan, X.; Xu, Z.; Wang, H.; Olsen, B. C.; Holt, C. M. B.; Mitlin, D. Carbonized chicken eggshell membranes with 3D architecture as high-performance electrode materials for supercapacitors. *Adv. Energy Mater.* **2012**, *2*, 431–437.
37. Stoller, M. D.; Ruoff, R. S. Best practice methods for determining an electrode material's performance for ultracapacitors. *Energy Environ. Sci.* **2010**, *3*, 1294–1301.
38. Agnihotri, S.; Rood, M. J.; Rostam-Abadi, M. Adsorption equilibrium of organic vapors on single-walled carbon nanotubes. *Carbon* **2005**, *43*, 2379–2388.
39. Sui, Z.-Y.; Meng, Q.-H.; Li, J.-T.; Zhu, J.-H.; Cui, Y.; Han, B.-H. High surface area porous carbons produced by steam activation of graphene aerogels. *J. Mater. Chem. A* **2014**, *2*, 9891–9898.
40. Lillo-Ródenas, M. A.; Cazorla-Amorós, D.; Linares-Solano, A. Behaviour of activated carbons with different pore size distributions and surface oxygen groups for benzene and toluene adsorption at low concentrations. *Carbon* **2005**, *43*, 1758–1767.
41. Liang, Y.; Wu, D.; Fu, R. Carbon microfibers with hierarchical porous structure from electrospun fiber-like natural biopolymer. *Sci. Rep.* **2013**, *3*, 1119.
42. Luo, L.; Ramirez, D.; Rood, M. J.; Grevillot, G.; Hay, K. J.; Thurston, D. L. Adsorption and electrothermal desorption of organic vapors using activated carbon adsorbents with novel morphologies. *Carbon* **2006**, *44*, 2715–2723.
43. Ben, T.; Ren, H.; Ma, S.; Cao, D.; Lan, J.; Jing, X.; Wang, W.; Xu, J.; Deng, F.; Simmons, J. M.; Qiu, S.; Zhu, G. Targeted synthesis of a porous aromatic framework with high stability and exceptionally high surface area. *Angew. Chem. Int. Ed.* **2009**, *48*, 9457–9460.
44. Ren, H.; Ben, T.; Sun, F.; Guo, M.; Jing, X.; Ma, H.; Cai, K.; Qiu, S.; Zhu, G. Synthesis of a porous aromatic framework for adsorbing organic pollutants applications. *J. Mater. Chem.* **2011**, *21*, 10348–10353.
45. Yuan, Y.; Sun, F.; Ren, H.; Jing, X.; Wang, W.; Ma, H.; Zhao, H.; Zhu, G. Targeted synthesis of a porous aromatic framework with a high adsorption capacity for organic molecules. *J. Mater. Chem.* **2011**, *21*, 13498–13502.
46. Wu, D.; Nese, A.; Pietrasik, J.; Liang, Y.; He, H.; Kruk, M.; Huang, L.; Kowalewski, T.; Matyjaszewski, K. Preparation of polymeric nanoscale networks from cylindrical molecular bottlebrushes. *ACS Nano* **2012**, *6*, 6208–6214.
47. Chen, Q.; Liu, D.-P.; Zhu, J.-H.; Han, B.-H. Mesoporous conjugated polycarbazole with high porosity via structure tuning. *Macromolecules* **2014**, *47*, 5926–5931.
48. Feng, L.-J.; Chen, Q.; Zhu, J.-H.; Liu, D.-P.; Zhao, Y.-C.; Han, B.-H. Adsorption performance and catalytic activity of porous conjugated polyporphyrins via carbazole-based oxidative coupling polymerization. *Polym. Chem.* **2014**, *5*, 3081–3088.
49. Feng, L.-J.; Guo, J.-W.; Sun, Z.-Y. Spirobixanthene-based microporous polymeric microsphere for gas uptake and vapor adsorption. *Mater. Lett.* **2014**, *116*, 120–122.

50. Xu, F.; Xian, S.; Xia, Q.; Li, Y.; Li, Z. Effect of textural properties on the adsorption and desorption of toluene on the metal-organic frameworks HKUST-1 and MIL-101. *Adsorp. Sci. Tech.* **2013**, *31*, 325–339.
51. Qin, W.; Cao, W.; Liu, H.; Li, Z.; Li, Y. Metal-organic framework MIL-101 doped with palladium for toluene adsorption and hydrogen storage. *RSC Adv.* **2014**, *4*, 2414–2420.
52. Hou, L.; Lin, Y.-Y.; Chen, X.-M. Porous metal-organic framework based on μ_4-oxo tetrazinc clusters: sorption and guest-dependent luminescent properties. *Inorg. Chem.* **2008**, *47*, 1346–1351.
53. Xue, D.-X.; Lin, Y.-Y.; Cheng, X.-N.; Chen, X.-M. A tetracarboxylate-bridged dicopper(II) paddle-wheel-based 2-D porous coordination polymer with gas sorption properties. *Cryst. Growth Des.* **2007**, *7*, 1332–1336.
54. Wang, S.; Li, W.-C.; Zhang, L.; Jin, Z.-Y.; Lu, A.-H. Polybenzoxazine-based monodisperse carbon spheres with low-thermal shrinkage and their CO_2 adsorption properties. *J. Mater. Chem. A* **2014**, *2*, 4406–4412.
55. Ludwinowicz, J.; Jaroniec, M. Potassium salt-assisted synthesis of highly microporous carbon spheres for CO_2 adsorption. *Carbon* **2015**, *82*, 297–303.
56. Wahby, A.; Ramos-Fernández, J. M.; Martínez-Escandell, M.; Sepúlveda-Escribano, A.; Silvestre-Albero, J.; Rodríguez-Reinoso, F. High-surface-area carbon molecular sieves for selective CO_2 adsorption. *ChemSusChem* **2010**, *3*, 974–981.
57. Wickramaratne, N. P.; Jaroniec, M. Importance of small micropores in CO_2 capture by phenolic resin-based activated carbon spheres. *J. Mater. Chem. A* **2013**, *1*, 112–116.
58. Presser, V.; McDonough, J.; Yeon, S.-H.; Gogotsi, Y. Effect of pore size on carbon dioxide sorption by carbide derived carbon. *Energy Environ. Sci.* **2011**, *4*, 3059–3066.
59. Cinke, M.; Li, J.; Bauschlicher Jr., C. W.; Ricca, A.; Meyyappan, M. CO_2 adsorption in single-walled carbon nanotubes. *Chem. Phys. Lett.* **2003**, *376*, 761–766.
60. Sun, Y.; Wang, Y.; Zhang, Y.; Zhou, Y.; Zhou, L. CO_2 sorption in activated carbon in the presence of water. *Chem. Phys. Lett.* **2007**, *437*, 14–16.
61. López, M. C. B.; Martínez-Alonso, A.; Tascón, J. M. D. N_2 and CO_2 adsorption on activated carbon fibres prepared from Nomex chars. *Carbon* **2000**, *38*, 1177–1182.
62. Lozano-Castelló, Cazorla-Amorós, D.; Linares-Solano, A. Usefulness of CO_2 adsorption at 273 K for the characterization of porous carbons. *Carbon* **2004**, *42*, 1233–1242.
63. Wickramaratne, N. P.; Xu, J.; Wang, M.; Zhu, L.; Dai, L.; Jaroniec, M. Nitrogen enriched porous carbon spheres: attractive materials for supercapacitor electrodes and CO_2 adsorption. *Chem. Mater.* **2014**, *26*, 2820–2828.
64. Wang, H.; Gao, Q.; Hu, J. High hydrogen storage capacity of porous carbons prepared by usig activated carbon. *J. Am. Chem. Soc.* **2009**, *131*, 7016–7022.
65. Cheng, F.; Liang, J.; Zhao, J.; Tao, Z.; Chen, J. Biomass waste-derived microporous carbons with controlled texture and enhanced hydrogen uptake. *Chem. Mater.* **2008**, *20*, 1889–1895.
66. Yang, S. J.; Kim, T.; Im, J. H.; Kim, Y. S.; Lee, K.; Jung, H.; Park, C. R. MOF-derived hierarchically porous carbon with exceptional porosity and hydrogen storage capacity. *Chem. Mater.* **2012**, *24*, 464–470.
67. Nijkamp, M. G.; Raaymakers, J. E. M. J.; van Dillen, A. J.; de Jong, K. P. Hydrogen storage using physisorption – materials demands. *Appl. Phys. A: Mater. Sci. Process.* **2001**, *72*, 619–623.

68. Gogotsi, Y.; Dash, R. K.; Yushin, G.; Yildirim, T.; Laudisio, G.; Fischer, J. E. Tailoring of nanoscale porosity in carbide-derived carbons for hydrogen storage. *J. Am. Chem. Soc.* **2005**, *127*, 16006–16007.
69. Ansón, A.; Callejas, M. A.; Benito, A. M.; Maser, W. K.; Izquierdo, M. T.; Rubio, B.; Jagiello, J.; Thommes, M.; Parra, J. B.; Martínez, M. T. Hydrogen adsorption studies on single wall carbon nanotubes. *Carbon* **2004**, *42*, 1243–1248.
70. Sevilla, M.; Roulston, R.; Mokaya, R. Superactivated carbide-derived carbons with high hydrogen storage capacity. *Energy Environ. Sci.* **2010**, *3*, 223–227.
71. Jiang, H.-L.; Liu, B.; Lan, Y.-Q.; Kuratani, K.; Akita, T.; Shioyama, H.; Zong, F.; Xu, Q. From metal-organic framework to nanoporous carbon: toward a very high surface area and hydrogen uptake. *J. Am. Chem. Soc.* **2011**, *133*, 11854–11857.
72. Böttger-Hiller, F.; Kempe, P.; Cox, G.; Panchenko, A.; Janssen, N.; Petzold, A.; Thurn-Albrecht, T.; Borchardt, L.; Rose, M.; Kaskel, S.; Georgi, C.; Lang, H.; Spange, S. Twin polymerization at spherical hard templates: an approach to size-adjustable carbon hollow spheres with micro- or mesoporous shells. *Angew. Chem. Int. Ed.* **2013**, *52*, 6088–6091.